Nuclear Instruments and Methods in Physics Research A 334 (1993) 313–324
North-Holland

NUCLEAR
INSTRUMENTS
& METHODS
IN PHYSICS
RESEARCH
Section A

Spin-exchange collisions and their consequences for spin-polarized gas targets of hydrogen and deuterium

T. Walker and L.W. Anderson
Department of Physics, University of Wisconsin-Madison, Madison, WI 53706, USA

Received 8 February 1993

The effects of spin-exchange collisions on the polarization of dense spin-polarized samples of hydrogen and deuterium are analyzed. It is shown that even in large magnetic fields spin-exchange collisions transfer angular momentum between the electrons and the nuclei. This effect has important implications for the operation of densed spin-polarized targets and sources of hydrogen and deuterium. For tensor polarized targets care will be required to obtain a high tensor polarization, especially at low fields. For the specific case of sources that are spin-polarized by spin-exchange collisions with optically pumped alkali atoms, spin-exchange not only polarizes the hydrogen and deuterium electron spins, but polarizes the nuclear spins as well. For high-density vector-polarized targets this may eliminate the need for rf transitions to polarize the nuclei.

1. Introduction

Spin-exchange collisions have long been used to produce electron- and nuclear-spin-polarized samples of atoms that cannot be conveniently polarized by direct optical pumping [1]. While the basic origin of spin-exchange is well-understood [2], there are features of these collisions that involve the roles of nuclear spins, external magnetic fields, and time-scales for production of a spin-temperature distribution that are not widely appreciated. These important effects are not only fundamentally interesting but have significant consequences for applications of spin-exchange such as the production of a spin-polarized deuterium target [3] for scattering experiments. In this paper we analyze hydrogen/deuterium spin-exchange collisions with the aim of developing insights into the roles the above-mentioned effects play in spin-polarized targets.

When two atoms with antiparallel electron spins make a strong collision (in the sense of Purcell and Field [2]), the large difference in the molecular energies for spin singlet and triplet potential curves causes both spins to flip with about 50% probability for collisions at thermal velocity. Thus the cross sections for spin-exchange are large, 10^{-15}–10^{-14} cm^2. Since the molecular energy difference is typically an eV or more, the relatively weak hyperfine interactions and magnetic fields have negligible effect on the collisions at temperatures above a few K. Between collisions, however, the electron and nuclear spins precess about each other and about the external magnetic field. As a result, in the limit of rapid spin exchange the system reaches spin-temperature equilibrium [4]. This is true independent of the size of the external magnetic field. Of course, the rate at which the system approaches equilibrium is extremely important in determining whether a spin-temperature adequately describes the state of the system. For hydrogen atoms in a large magnetic field the time constant for the approach to equilibrium is

$$T_{\mathrm{ST}} = \left(1 + \left(\frac{g_{\mathrm{s}}\mu_{\mathrm{B}}B}{\delta\nu_{\mathrm{HFS}}}\right)^2\right) T_{\mathrm{H}} = (1+x^2)T_{\mathrm{H}}, \tag{1}$$

where $\delta\nu_{\mathrm{HFS}}$ is the ground-state hyperfine splitting in zero magnetic field, g_{s} is the electron g-factor, μ_{B} is the Bohr magneton, B is the magnetic field, $x = g_{\mathrm{s}}\mu_{\mathrm{B}}B/\delta\nu_{\mathrm{HFS}}$ is the Breit–Rabi field parameter, and $T_{\mathrm{H}}^{-1} = n_{\mathrm{H}}\langle\sigma s_{\mathrm{se}}(\mathrm{HH})v\rangle$ is the thermally averaged hydrogen–hydrogen spin-exchange rate. Eq. (1) is

approximately true for deuterium as well. Thus in a large magnetic field the rate of relaxation to spin-temperature equilibrium is considerably smaller due to the reduced coupling of the electron to the nucleus. However, if many collisions occur substantial angular momentum may still be transferred between the electron and the nucleus.

The physical effects represented by eq. (1) have profound significance for the production of dense vector-polarized targets of hydrogen and deuterium, and tensor-polarized deuterium [5]. First, for hydrogen in non-zero magnetic fields and deuterium in any field spin-exchange collisions will transfer angular momentum between the electrons and the nuclei. Second, the tensor polarization of deuterium targets is strongly modified by spin-exchange collisions, especially at low fields. In the limit of many spin-exchange collisions the tensor polarization must be positive. Third, for targets and sources produced by the optical pumping/spin-exchange technique [3] the deuterium and hydrogen nuclei can be directly polarized by spin-exchange. For vector-polarized targets this may lead to a substantial simplification of the apparatus, since rf transitions are not necessary. If one desires to obtain negative tensor-polarized targets, then care must be taken to mimimize spin-exchange collisions, since, as shown in section 3, in the spin-temperature limit the tensor polarization is always positive, with the value of the tensor polarization being determined by the total angular momentum stored in the atom.

In section 2 we present analytical results for H–H spin exchange in arbitrary fields. In section 3 we present numerical calculations for D–D spin-exchange, including the effects of tensor polarization. In section 4, we treat the important case of spin-exchange optical pumping, with the inclusion of alkali-H spin exchange collisions together with H–H collisions and show that the H nuclei become polarized even in a large magnetic field. Here we make approximate extensions to alkali-D spin-exchange as well. In section 5 we show how the processes under consideration affect the polarized deuterium target of Coulter et al. [3] (from now on, referred to as the Argonne target). In section 6 we discuss the consequences of these results for spin-polarized hydrogen and deuterium targets.

2. H–H spin-exchange in arbitrary fields

We consider hydrogen–hydrogen spin-exchange collisions in arbitrary magnetic fields. For reference, the energy levels for hydrogen in a magnetic field are shown in fig. 1. The states are $|1\rangle = |\uparrow \tfrac{1}{2}\rangle$, $|2\rangle = \cos\theta\,|\uparrow -\tfrac{1}{2}\rangle + \sin\theta\,|\downarrow \tfrac{1}{2}\rangle$, $|3\rangle = -\sin\theta\,|\uparrow -\tfrac{1}{2}\rangle + \cos\theta\,|\downarrow \tfrac{1}{2}\rangle$, $|4\rangle = |\downarrow -\tfrac{1}{2}\rangle$. Here the arrows denote the projection of the electron spin along the direction of the magnetic field, and $\pm\tfrac{1}{2}$ are the

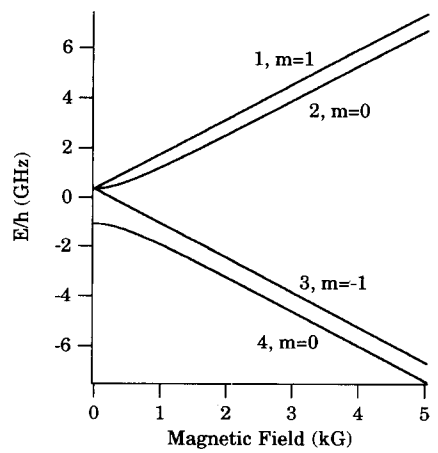

Fig. 1. Energy levels for H in a magnetic field. The levels are labelled by the numbers used in the text, and their component of total angular momentum along the magnetic field direction.

projections of the proton spin along the magnetic field direction. The magnetic-field dependent mixing angle θ is given by $\tan 2\theta = \delta\nu_{\mathrm{HFS}}/g_s\mu_B B = 1/x$. Spin-exchange causes the atoms to change states consistent with conservation of the z-component of the angular momentum. An example of a possible spin-exchange reaction is $|1\rangle + |2\rangle \rightarrow |1\rangle + |4\rangle$.

We assume that the system is adequately described by only considering the populations $P_1 \ldots P_4$, and ignoring coherences. This is adequate for our purposes, since we are not concerned with effects involving coherence such as frequency shifts [6]. The rate equations for the populations are derived using the method of Purcell and Field [2]. It can be shown that the resulting rate equations are

$$T_{\mathrm{H}}\frac{\mathrm{d}P_1}{\mathrm{d}t} = P_2P_4 - P_1P_3 + \frac{\sin^2 2\theta}{4}(P_2 - P_4)^2, \tag{2}$$

$$T_{\mathrm{H}}\frac{\mathrm{d}P_2}{\mathrm{d}t} = P_1P_3 - P_2P_4 + \frac{\sin^2 2\theta}{2}\left(P_1P_4 - P_1P_2 - P_2P_3 + P_3P_4 + P_2P_4 + P_4^2/2 - 3P_2^2/2\right), \tag{3}$$

$$T_{\mathrm{H}}\frac{\mathrm{d}P_3}{\mathrm{d}t} = P_2P_4 - P_1P_3 + \frac{\sin^2 2\theta}{4}(P_2 - P_4)^2, \tag{4}$$

$$T_{\mathrm{H}}\frac{\mathrm{d}P_4}{\mathrm{d}t} = P_1P_3 - P_2P_4 + \frac{\sin^2 2\theta}{2}\left(-P_1P_4 + P_1P_2 + P_2P_3 - P_3P_4 + P_2P_4 - 3P_4^2/2 + P_2^2/2\right), \tag{5}$$

where $T_{\mathrm{H}}^{-1} = n_{\mathrm{H}}\langle\sigma_{\mathrm{se}}(\mathrm{HH})v\rangle$. Using $P_1 + P_2 + P_3 + P_4 = 1$ and $\langle F_z\rangle = P_1 - P_3$ the equations simplify considerably:

$$T_{\mathrm{H}}\frac{\mathrm{d}(P_2 - P_4)}{\mathrm{d}t} = -\sin^2 2\theta(P_2 - P_4), \tag{6}$$

$$T_{\mathrm{H}}\frac{\mathrm{d}(P_2 + P_4)}{\mathrm{d}t} = -(P_2 + P_4) + \frac{1 - \langle F_z\rangle^2}{2} + \frac{\cos^2 2\theta}{2}(P_2 - P_4)^2. \tag{7}$$

In steady state, $P_2 - P_4 = 0$ and the system can be characterized by a spin-temperature, with $P_1 = \mathrm{e}^{\beta}/N$, $P_2 = P_4 = 1/N$, $P_3 = \mathrm{e}^{-\beta}/N$, and $N = 4\cosh^2\beta/2$. The constant β is related to $\langle F_z\rangle$ by $\langle F_z\rangle = \tanh\beta/2$. Note that this distribution is independent of the strength of the magnetic field. This is because the collisions bring the system to an equilibrium that has the most probable distribution consistent with a given total z-component of angular momentum. The most probable distribution is one where there is a spin temperature. The magnetic field does not affect this distribution. A mathematical treatment of the magnetic-field independence of the spin-temperature distribution is given by Happer [6].

There are several consequences of the magnetic-field independence of the spin-temperature distribution. First, once the system reaches a spin-temperature distribution at any field, it remains in that distribution even if the field is changed. This is true even for arbitrary values of the nuclear spin. Second, for hydrogen in spin-temperature equilibrium the angular momentum is equally shared between the nuclear spin I_z and the electron spin S_z, i.e. $\langle S_z\rangle = \langle I_z\rangle = \langle F_z\rangle/2$. Again, this is valid independent of the field strength. We discuss further consequences of this for rf spectroscopy in section 6.

Of considerable importance for this work is the nature of the transient solution to eq. (6), which governs whether or not the system has reached the spin-temperature equilibrium. This solution is

$$P_2 - P_4 = (P_2 - P_4)_0 \exp\left(-t\,\sin^2 2\theta/T_{\mathrm{H}}\right), \tag{8}$$

where the subscript 0 indicates the initial condition. Thus the evolution of the system toward a spin-temperature distribution occurs with a time constant

$$T_{\mathrm{ST}} = \frac{T_{\mathrm{H}}}{\sin^2 2\theta} = (1 + x^2)T_{\mathrm{H}}. \tag{9}$$

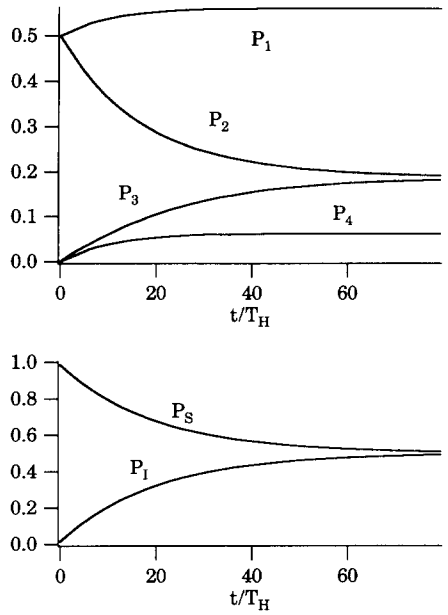

Fig. 2. Evolution of the populations and nuclear and electronic spin polarizations for H atoms undergoing H–H spin-exchange collisions in a 2.2kG magnetic field, with initial conditions $P_1 = P_2 = \frac{1}{2}$ corresponding to 100% electron spin polarization and 0% nuclear spin polarization.

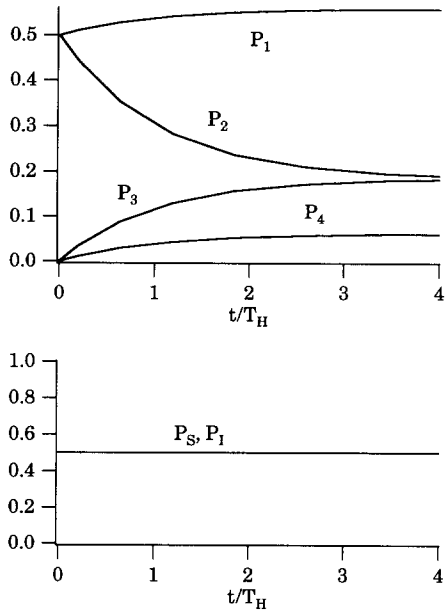

Fig. 3. Spin-exchange evolution in zero magnetic field, with the initial condition $P_1 = P_2 = \frac{1}{2}$.

For atoms with $I > \frac{1}{2}$, eq. (9) is still a useful approximation. An immediate consequence of eq. (9) is that in a given large magnetic field deuterium ($\delta\nu_{HFS} = 327$ MHz) will reach a spin-temperature distribution more than one order of magnitude slower than hydrogen ($\delta_{HFS} = 1420$ MHz).

In figs. 2 and 3 we show the time evolution (in units of the spin-exchange time T_H) of the populations of the various states of H, for magnetic fields of 2.2 and 0 kG. We also have plotted the electron and nuclear spin-polarizations as a function of time. For the 0 G case, an important feature peculiar to H–H spin-exchange is apparent. Since states $|2\rangle$ and $|4\rangle$ have $\langle S_z\rangle = \langle I_z\rangle = 0$ at zero field, the difference $P_1 - P_3$ solely determines the spin polarizations. Since this quantity is conserved in spin-exchange collisions, the collisions do not affect the spin polarizations, even though the state populations are changed. At high fields, this is no longer true and the collisions redistribute the angular momentum between the electron and nuclear spins.

To summarize, H–H spin-exchange collisions bring about a spin-temperature distribution in which the angular momentum is shared between the electron and nucleus. At large magnetic fields the rate at which the system approaches this spin temperature is slowed by the field. In very dense polarized vapors at non-zero magnetic fields, however, it may be possible to have substantial modification of the nuclear polarization due to the large numbers of spin-exchange collisions.

3. D–D spin-exchange in arbitrary fields

For atoms with nuclear spin $I > \frac{1}{2}$ the spin-exchange equations analogous to eqs. (2)–(5) become much more complicated. In this section we give a straightforward, general method for generating these equations, again ignoring coherences, and discuss the numerical solutions.

The energy levels for D are shown in fig. 4. The magnetic field dependent states are $|1\rangle = |\uparrow 1\rangle$, $|2\rangle = \cos\theta + |\uparrow 0\rangle + \sin\theta + |\downarrow 1\rangle$, $|3\rangle = \cos\theta - |\uparrow -1\rangle + \sin\theta - |\downarrow 0\rangle$, $|4\rangle = |\downarrow 01\rangle$, $|5\rangle = -\sin\theta - |\uparrow -1\rangle + \cos\theta_- |\downarrow 0\rangle$, and $|6\rangle = -\sin\theta_+ |\uparrow 0\rangle + \cos\theta_+ |\downarrow 1\rangle$. Here the magnetic-field-dependent

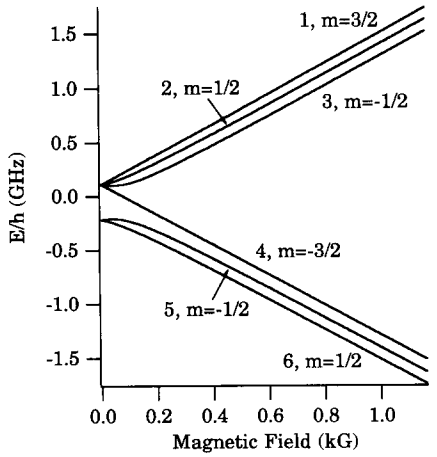

Fig. 4. Energy levels for D in a magnetic field. The levels are labelled by the numbers used in the text, and their component of total angular momentum along the magnetic field direction.

mixing angles obey $\tan\theta = \sqrt{8}/(3x \pm 1)$. In the following, when refering to a general state $|q\rangle$, we use the notation $|q\rangle = q_\uparrow |\uparrow m_q - 1\rangle + q_\downarrow |\downarrow m_q + 1\rangle$, where $m_q = \langle q | F_z | q \rangle$.

Again using the method of Purcell and Field [2], we have

$$T_D \dot{P}_c = \sum_{ab} M^c_{ab} P_a P_b, \tag{10}$$

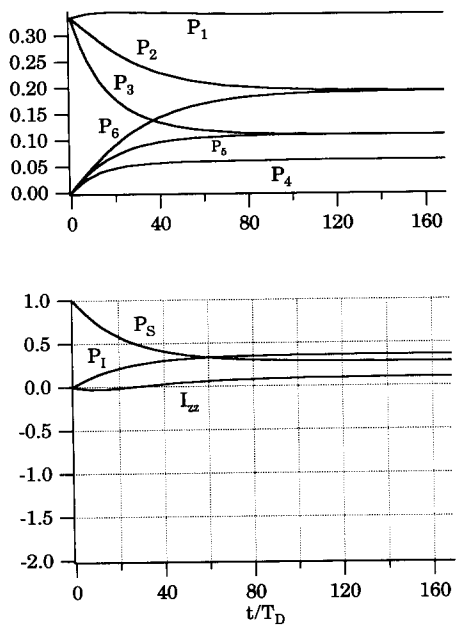

Fig. 5. Evolution of the populations of the D states, the electron and nuclear spin polarizations, and the nuclear tensor polarization for D atoms undergoing D–D spin-exchange collisions. The initial conditions are $P_1 = P_2 = P_3 = \frac{1}{3}$, and the magnetic field is 500 G.

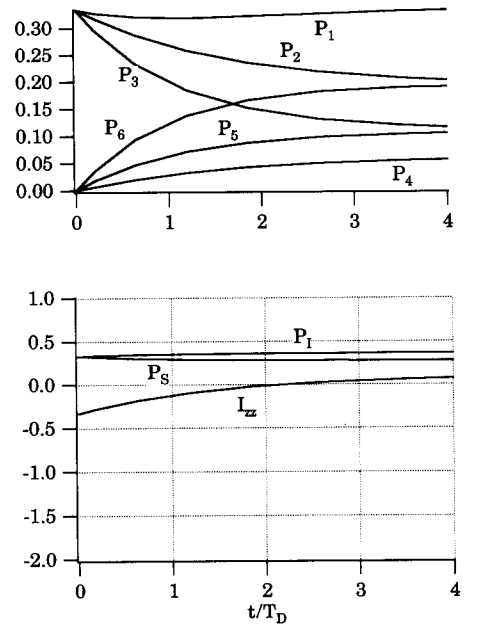

Fig. 6. The same as fig. 5 except zero magnetic field.

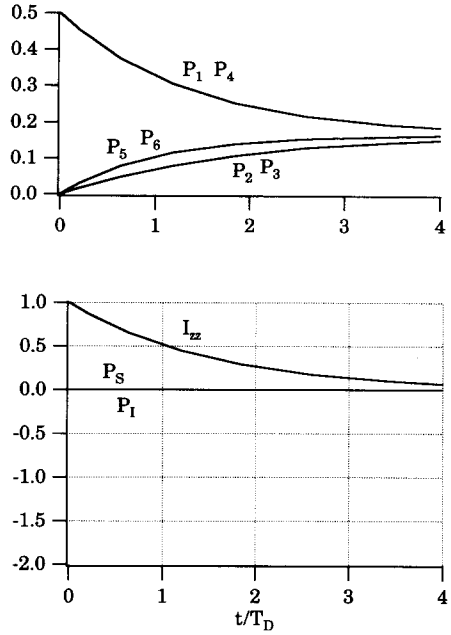

Fig. 7. Zero-magnetic field evolution of the populations and polarizations of initially $I_{zz} = +1$ tensor polarized D, with assumed initial conditions shown.

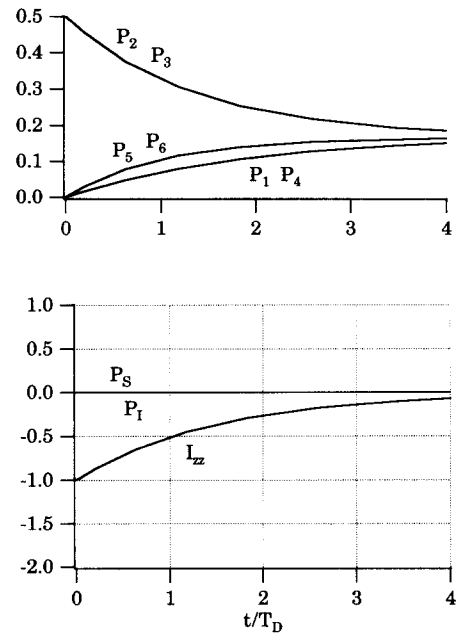

Fig. 8. The same as fig. 7 except $I_{zz} = -1$.

where it is shown in Appendix A that the coefficients M^c_{ab} are given by

$$M^c_{ab} = \sum_d \Big(-\langle c \mid a\rangle\langle d \mid b\rangle (a_\uparrow b_\downarrow c_\uparrow d_\downarrow + a_\downarrow b_\uparrow c_\downarrow d_\uparrow)$$
$$+ \langle m_c \mid m_a\rangle\langle m_d \mid m_b\rangle (a_\uparrow b_\downarrow c_\uparrow d_\downarrow + a_\downarrow b_\uparrow c_\downarrow d_\uparrow)^2/2$$
$$+ \langle m_c \mid m_a - 1\rangle\langle m_d \mid m_b + 1\rangle (a_\uparrow b_\downarrow c_\downarrow d_\uparrow)^2/2$$
$$+ \langle m_c \mid m_a + 1\rangle\langle m_d \mid m_b - 1\rangle (a_\downarrow b_\uparrow c_\uparrow d_\downarrow)^2/2\Big). \qquad (11)$$

Note that the magnetic field dependence is contained in the various coefficients $q_\uparrow$ and $q_\downarrow$. In figs. 5–9 we show solutions to these equations for various initial conditions and magnetic fields.

In fig. 5 we consider the initial conditions $P_1 = P_2 = P_3 = \frac{1}{3}$, corresponding to D atoms 100% electron-spin-polarized by a high-field sextupole magnet. Note that the spin-exchange collisions transfer the electron spin-polarization to the nucleus, but in the 500 G magnetic field the number of collisions required is quite large. In fig. 6 the same situation is shown, but the atoms are assumed to pass adiabatically into a small field before any collisions occur. In this case, the hyperfine interaction directly transfers angular momentum from the electron to the nucleas as the atoms adiabatically follow the Breit–Rabi curves of fig. 4. While the spin-exchange collisions make only a small additional effect on the nuclear polarization, note that if the atoms were to reenter subsequently a strong field region the electron spin-polarization would be only approximately 28%.

Figs. 7–9 show how deuterium atoms that are purely tensor polarized evolve due to spin-exchange. In particular note that the tensor polarization in spin-temperature equilibrium is always positive, even if the initial tensor polarization is negative. In the spin-temperature limit, the tensor polarization depends only on the total angular momentum, as shown in fig. 10. For a given number of collisions, the degradation of the tensor polarization is slowed at high fields.

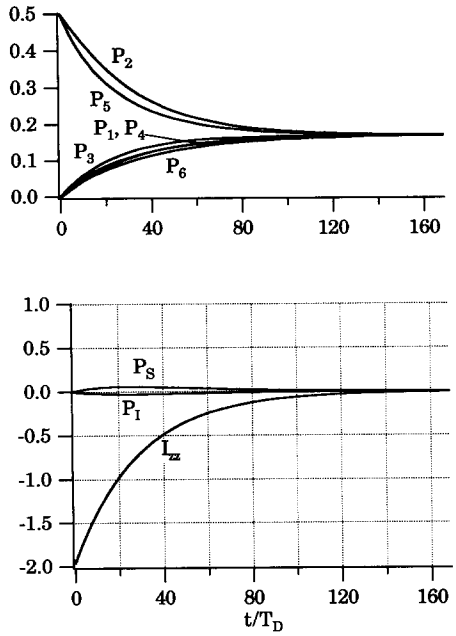

Fig. 9. The same as fig. 7 except $J_{zz} = -2$ and a 500 G magnetic field.

4. Spin-exchange optical pumping in large magnetic fields

In the previous sections we showed how H–H and D–D spin-exchange collisions bring about substantial polarization of the nuclei even in large magnetic fields. Of considerable current interest is the technique of spin-exchange optical pumping. Thus in this section we consider spin-exchange collisions in the presence of an optically pumped alkali (A) vapor in a large magnetic field. We show that the combined effects of A–H and H–H collisions are to polarize the H nuclei as well as the H electrons provided the H–H collision rate is sufficiently high. Here the rate T_{ST}^{-1} that the H atoms come to spin-temperature equilibrium again plays a vital role. To summarize, substantial amounts of angular momentum can be stored in the H (or D) nuclei if H–H (or D–D) spin-exchange collision rates are high.

We perform the calculations exactly for hydrogen and make approximate extensions for deuterium. Since a large magnetic field is necessary for efficient optical pumping of the A atoms [7–9], we restrict

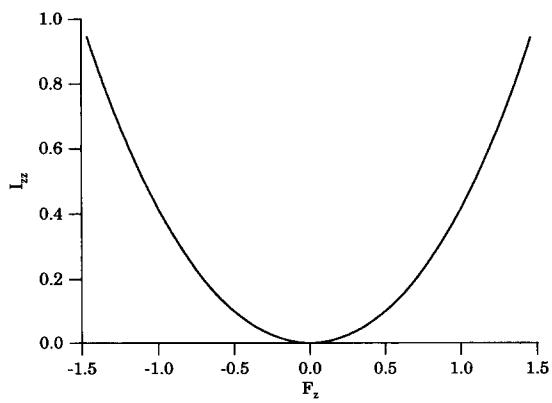

Fig. 10. Value of the tensor polarization I_{zz} as a function of the total angular momentum $F_z = S_z + I_z$, in the spin-temperature limit.

the calculations to large magnetic fields. In addition, we assume that the optical pumping rate of the alkali atoms is large enough that relaxation of the alkali spins by spin exchange is negligible. We assume the spin-relaxation rate (on the walls, for example) of either the alkali or hydrogen spins is negligible. The rate equations are again obtained with the method of Purcell and Field [2]. In high field, we have $\langle I_z\rangle \approx (P_1 - P_2 - P_3 + P_4)/2$ and so the relevant equations for A–H and H–H spin exchange can be written as

$$\frac{\mathrm{d}\langle F_z\rangle}{\mathrm{d}t} = \frac{1}{T_A}\left(P_A/2 - \langle F_z\rangle + \langle I_z\rangle\right), \tag{12}$$

$$\frac{\mathrm{d}\langle I_z\rangle}{\mathrm{d}t} = \frac{1}{2T_{ST}}\left(\langle F_z\rangle - 2\langle I_z\rangle\right), \tag{13}$$

where P_A is the alkali electron spin polarization and where $T_A = n_A\langle\sigma_{se}(\mathrm{KH})v\rangle$ is the thermally averaged alkali-hydrogen spin-exchange rate.

In equilibrium, we have $\langle F_z\rangle = P_A$ and $\langle I_z\rangle = P_A/2$ so that the polarizations of the hydrogen electron and nuclear spins become equal to the alkali spin polarization. At high field, however, the critical issue is at what rate the system approaches this equilibrium. The transient solutions to the above equations are exponentials with rate constants

$$\lambda_{\pm} = \frac{1}{2T_A} + \frac{1}{2T_{ST}} \pm \sqrt{\left(\frac{1}{2T_A}\right)^2 + \left(\frac{1}{2T_{ST}}\right)^2}\,. \tag{14}$$

An interesting special case is the limit $T_{ST} \gg T_A$. This corresponds to the situation where the hydrogen electron spin-polarization is in spin-exchange equilibrium with the alkali electron spin-polarization. Then the transient behaviors of $\langle I_z\rangle$ and $\langle F_z\rangle$ are

$$\langle F_z\rangle = \frac{P_A}{2} + \langle I_z\rangle, \tag{15}$$

$$\langle I_z\rangle = \frac{P_A}{2}\left(1 - \exp\frac{-t}{2T_{ST}}\right). \tag{16}$$

This says that the hydrogen electron spin is quickly polarized to a value $P_A/2$, and the nuclear spin is then slowly polarized by repeated H–H spin-exchange collisions.

For deuterium we expect similar behavior, i.e.

$$\frac{\mathrm{d}\langle F_z\rangle}{\mathrm{d}t} = \frac{1}{T_A}\left(P_A/2 - \langle F_z\rangle + \langle I_z\rangle\right), \tag{17}$$

$$\frac{\mathrm{d}\langle I_z\rangle}{\mathrm{d}t} = -\frac{1}{2T_{ST}}\left(\langle F_z\rangle - \tfrac{3}{2}\langle I_z\rangle\right). \tag{18}$$

In the limit of $T_{ST} \gg T_A$, the transient solutions are

$$\langle F_z\rangle = \frac{P_A}{2} + \langle I_z\rangle, \tag{19}$$

$$\langle I_z\rangle = P_A\left(1 - \exp\frac{-t}{4T_{ST}}\right). \tag{20}$$

In section 5 we will show that these equations imply that spin-exchange collisions partially polarize the D nuclei under the conditions of the Argonne-polarized target.

5. Application to the Argonne spin-polarized deuterium target

The Argonne source of deuterium atoms [3] is a high-density source in which deuterium atoms are polarized by spin-exchange collisions with optically-pumped potassium atoms. A rf dissociator produces D atoms that flow at a rate that is typically 2.7×10^{17} atoms/s (atomic fraction of 0.65 × total flow of 4.2×10^{17} nuclei/s) into a cylindrical cell (2.2 cm diameter × 4.5 cm length) which is heated to 513 K and contains potassium vapor at a density of 1.7×10^{12} cm^{-3}. The potassium is optically pumped by absorption of circularly polarized light from a Ti:sapphire laser operating at the wavelength for the $4^2S_{1/2} \rightarrow 4^2P_{1/2}$ transition. The potassium electron spin-polarization is measured by absorption of a weak probe laser. A large magnetic field (2–4 kG) is applied to the cell to minimize the depolarizing effects of radiation trapping [7–9] which would normally prevent optical pumping at these densities. Deuterium atoms in the cell are polarized by spin-exchange collisions with the polarized K atoms. The density of the D atoms in the cell at the above flow rate is 1.1×10^{14} cm^{-3}. The atoms flow out of the cell through a 0.28 cm diameter hole and into a drifilm-coated exit tube (1.9 cm diameter × 27.6 cm length). The magnetic field in this region is typically 40 G. After leaving the exit tube a small fraction of the D atoms enter a sextupole magnet that is used to measure the electron spin-polarization of the D atoms.

We estimate the spin-exchange rates in the apparatus. Using a cross section of $\sigma_{se}(DD) = 2 \times 10^{-15}$ cm^2 [10,11] for D–D spin exchange, the calculated spin-exchange rate in the optical pumping cell is $1/T_D = n_D \langle \sigma_{se}(DD) v \rangle = 8.0 \times 10^4$ s^{-1}. At a typical potassium density of 10^{12} cm^{-3}, the K–D spin exchange rate is $1/T_K = n_K \langle \sigma_{se}(KD) v \rangle = 1.9 \times 10^3$ s^{-1} where we have used a cross section of $\sigma_{se}(KD) = 7.4 \times 10^{-15}$ cm^2 [12]. Thus D–D collisions take place at a much higher rate than D–K collisions. We also need to estimate the total number of spin-exchange collisions an average D atom experiences before leaving the optical pumping cell. The dwell time of 6.9 ms in the cell is determined from the number of atoms in the cell divided by the flow rate. A given D atom makes therefore on the average 550 D–D spin-exchange collisions and 13 D–K spin-exchange collisions while in the optical pumping cell. Thus many D–K and D–D spin-exchange collisions occur before the atoms exit the cell.

Spin-exchange collisions are not negligible in the exit tube, either. We estimate the density profile in the exit tube by assuming the density decreases linearly from its value just after the hole that connects the tube to the optical pumping cell to zero at the end of the exit tube. The density just downstream from the hole between the cell and the tube is reduced from the density in the cell by the factor $1 + C_{tube}/C_{hole}$, where the C's are the conductances. Using standard formulae for these conductances, we estimate that the deuterium density just downstream from the hole is a factor of 5 smaller than in the cell, so the average density in the tube is a factor of 10 smaller than in the cell. The dwell time in the tube is equal to the number of atoms in the tube divided by the flow rate, giving a result of 3 ms. On the average a D atom makes more than 30 D–D spin-exchange collisions in the tube. Thus spin-exchange collisions are prevalent in the exit tube as well as in the optical pumping cell.

We now apply the results of the calculations of sections 2 and 4 to this experiment. In the optical pumping cell, the 2.2 kG magnetic field means that the rate for relaxation to a spin-temperature is quite slow:

$$\frac{1}{T_{ST}} = \frac{2.8 \times 10^{-3}}{T_D} = 210 \text{ s}^{-1}. \tag{21}$$

Using the 6.9 ms dwell time in the optical pumping cell, we find from eq. (20) and 19 that $\langle I_z \rangle = 0.3 P_K$ and $\langle F_z \rangle = 0.8\ P_K$ so due to the large number of spin-exchange collisions the nuclear spin is substantially polarized despite the large magnetic field.

In the exit tube, the magnetic field drops off to small values, so the estimated 30 spin-exchange collisions should be sufficient to bring the atoms to spin-temperature equilibrium. Then $P_I \approx P_S \sim 0.53 P_K$. The sextupole magnet measures P_s, so at high potassium densities a deuterium electron spin polarization

of 53% should be measured by the sextupole polarimeter. This is in reasonable agreement with recent measurements of about 60% by the Argonne group [13].

We note that the process of chemical exchange, which has been ignored here, may also play a role in the Argonne source since there are a significant number of D_2 molecules present.

6. Conclusions

We have demonstrated that spin-exchange collisions polarize the nuclei of hydrogen and deuterium even in large magnetic fields if the spin-exchange rates are large enough. In particular, the Argonne polarized target has sufficiently large collision rates that the effects discussed in this paper are important. For other current sources, such as storage cell targets, the number of collisions is smaller and the effects discussed here are likely to be observed only for deuterium at low magnetic fields. Of course, as the properties of these sources are improved, spin-exchange collisions will become important. In this section, we conclude by summarizing some of the ramifications of spin-exchange collisions for polarized targets in general and the Argonne target in particular.

First, since H–H spin-exchange collisions at low field do not change the vector polarization, spin-exchange should not affect these targets once the nuclei are polarized.

For D targets spin-exchange affects both the vector and tensor polarizations in all fields. Tensor polarizations are especially susceptible, and in the limit of large numbers of collisions the tensor polarization cannot be negative. Magnetic fields can be used to increase the number of collisions required to degrade the tensor polarization.

Spin-exchange not only affects the nuclear polarizations in the target but may also play a role in the production of the desired polarization. This is because spin-exchange collisions that occur before the atoms reach an rf transition region can redistribute the populations of the various levels. This occurs for either hydrogen and deuterium at all fields. In addition, spin-exchange causes shifts in the magnetic resonance frequencies, although we have not calculated these shifts in this paper.

The efficiency of the spin-exchange method for polarizing hydrogen will be much greater than for deuterium in the same magnetic field. Since the hydrogen hyperfine structure is a factor of 4 larger than deuterium, the coupling between the electron and nuclear spins will be much stronger (a factor of typically 20). Thus the proton spins will be very efficiently polarized in the spin exchange cell of the Argonne source at a magnetic field of 2.2 kG. In this case rf transitions are completely unnecessary since the proton has spin $\frac{1}{2}$ and tensor polarization is not possible. Very high proton polarizations should be attainable this way.

In general, it will be necessary for designs of high-density polarized H and D targets and sources to take into consideration the effects of spin-exchange collisions.

Acknowledgements

We are grateful to the Argonne group for illuminating discussions and for sharing their unpublished data that stimulated these calculations. We acknowledge the support of the NSF (Grant Numbers PHY-9005895 and PHY-9257058) and the University of Wisconsin Research Committee. T.W. is an Alfred P. Sloan Fellow.

Appendix

Derivation of rate equations

We apply the method of Purcell and Field [2] to calculate the general spin-exchange rate equations, eqs. (10) and (11), ignoring coherences but including hyperfine and magnetic field interactions. The two

colliding atoms begin a collision with the first atom in the state $|a\rangle = a_\uparrow |\uparrow m_a - \frac{1}{2}\rangle + a_\downarrow |\downarrow m_a + \frac{1}{2}\rangle$ and the second in the state $|b\rangle = b_\uparrow |\uparrow m_b - \frac{1}{2}\rangle + b_\downarrow |\downarrow m_b + \frac{1}{2}\rangle$, and we calculate the probability of the collision ending with the first atom in state $|c\rangle$ and the second in state $|d\rangle$. The arrows denote the projection of the electron spin along the magnetic field, and the other quantum number for the states is the projection of the nuclear spin along the magnetic field. The states $|a\rangle$, $|b\rangle$, $|c\rangle$, and $|d\rangle$ are eigenstates of the free atom Hamiltonian, including Zeeman and hyperfine interactions.

As a result of the collision, the initial state $|ab\rangle$ becomes the new state $U|a\rangle|b\rangle$, where $U = P_s + e^{-i\phi}P_t$ is the time evolution operator for the collision, P_s is the projection operator for electron spin singlet states, P_t is the projection operator for electron spin triplet states, and ϕ is the difference between the phase accumulations for the singlet and triplet curves. The probability of ending up in the final state $|c\rangle|d\rangle$ is $|\langle cd|U|ab\rangle|^2$. The time rate of change of the population P_c is then the total collision rate $2n\langle\sigma_{SE}v\rangle$ times the sum over all the states $|a\rangle$, $|b\rangle$, and $|d\rangle$ of the transition probabilities times the populations P_a and P_b. Thus the time evolution of the population P_c obeys

$$\dot{P}_c = 2n\langle\sigma_{SE}v\rangle \sum_{ab} \left[|\langle cd|U|ab\rangle|^2 - |\langle cd|ab\rangle|^2 \right] P_a P_b \tag{A.1}$$

$$= 2n\langle\sigma_{SE}v\rangle \sum_{ab} M^c_{ab} P_a P_b. \tag{A.2}$$

Using the projection operators, we find

$$\begin{aligned} U|ab\rangle = |ab\rangle - \frac{1 - e^{-i\phi}}{2} \\ \times \Big[a_\uparrow b_\downarrow \big(|\uparrow m_a - \tfrac{1}{2} \downarrow m_b + \tfrac{1}{2}\rangle - |\downarrow m_a - \tfrac{1}{2} \uparrow m_b + \tfrac{1}{2}\rangle \big) \\ - a_\downarrow b_\uparrow \big(|\uparrow m_a + \tfrac{1}{2} \downarrow m_b - \tfrac{1}{2}\rangle - |\downarrow m_a + \tfrac{1}{2} \uparrow m_b - \tfrac{1}{2}\rangle \big) \Big] \end{aligned} \tag{A.3}$$

and therefore

$$\begin{aligned} \langle cd|U|ab\rangle = \langle c|a\rangle\langle d|b\rangle + \frac{1 - e^{-i\phi}}{2} \\ \times \big[-a_\uparrow b_\downarrow c_\uparrow d_\downarrow \langle m_c|m_a\rangle\langle m_d|m_b\rangle + a_\uparrow b_\downarrow c_\downarrow d_\uparrow \langle m_c|m_a - 1\rangle\langle m_d|m_b + 1\rangle \\ + a_\downarrow b_\uparrow c_\uparrow d_\downarrow \langle m_c|m_a + 1\rangle\langle m_d|m_b - 1\rangle - a_\downarrow b_\uparrow c_\downarrow d_\uparrow \langle m_c|m_a\rangle\langle m_d|m_b\rangle \big]. \end{aligned} \tag{A.4}$$

Averaging over the assumed random distribution of ϕ, we then obtain

$$\begin{aligned} M^c_{ab} = \sum_d \Big(-\langle c|a\rangle\langle d|b\rangle (a_\uparrow b_\downarrow c_\uparrow d_\downarrow + a_\downarrow b_\uparrow c_\downarrow d_\uparrow) \\ + \langle m_c|m_a\rangle\langle m_d|m_b\rangle (a_\uparrow b_\downarrow c_\uparrow d_\downarrow + a_\downarrow b_\uparrow c_\downarrow d_\uparrow)^2/2 \\ + \langle m_c|m_a - 1\rangle\langle m_d|m_b + 1\rangle (a_\uparrow b_\downarrow c_\downarrow d_\uparrow)^2/2 \\ + \langle m_c|m_a + 1\rangle\langle m_d|m_b - 1\rangle (a_\downarrow b_\uparrow c_\uparrow d_\downarrow)^2/2 \Big) \end{aligned} \tag{A.5}$$

which is eq. (11).

References

[1] L.W. Anderson, F.M. Pipkin and J.C. Baird, Phys. Rev. Lett. 1 (1958) 229.

[2] E.M. Purcell and G.B. Field, Astrophys. J. 124 (1956) 542.

[3] K. Coulter, R. Holt, E. Kinney, R. Kowalczyk, D. Potterveld, L. Young, B. Zeidman, A. Zghiche and D. Toporkov, Phys. Rev. Lett. 68 (1992) 174.

[4] L.W. Anderson, F.M. Pipkin and J.C. Baird, Phys. Rev. Lett. 4 (1960) 69.
[5] T. Walker and L.W. Anderson, to be published.
[6] W. Happer, Rev. Mod. Phys. 44 (1972) 169.
[7] D. Tupa, L.W. Anderson, D.L. Huber and J.E. Lawler, Phys. Rev. A33 (1986) 1045.
[8] D. Tupa and L.W. Anderson, Phys. Rev. A36 (1987) 2142.
[9] L.W. Anderson and T. Walker, Nucl. Instr. and Meth. A316 (1992) 123.
[10] D.R. Swenson, D. Tupa and L.W. Anderson, J. Phys. B: At. Mol. Phys. 18 (1985) 4433.
[11] J. Koelman, S. Crampton, H. Stoof, O. Luiten and B. Verhaar, Phys. Rev. A38 (1988) 3535.
[12] H.R. Cole and R.E. Olson, Phys. Rev. A31 (1985) 2137.
[13] D. Toporkov, private communication.